Korean J. of Chem. Eng., **7**(3) (1990) 210-218

SEPARATION OF CLOSE-BOILING COMPONENTS BY THE COMBINED CONTINUOUS AND PREPARATIVE CHROMATOGRAPHY: COMPARISON OF EXPERIMENTAL DATA WITH CALCULATED VALUES IN BINARY SYSTEM

Kyung Ho ROW*, Youn Yong LEE and Won Kook LEE**

Separation Process Lab., Division of Chemical Engineering, Korea Institute of Science and Technology, P.O. Box 131, Cheongryang, Seoul, Korea

**Department of Chemical Engineering, Korea Advanced Institute of Science and Technology, P.O. Box 150, Cheongryang, Seoul, Korea

(Received 11 April 1990 • accepted 29 June 1990)

Abstract—Operational characteristics of the combined continuous and preparative gas-liquid chromatographic system were investigated for the separation of two close-boiling components, diethylether and dichloromethane. It was experimentally confirmed that the additional column length and the desorbent velocity were the most important factors to ensure the continuous separation of the feed mixture.

The theoretical concentration profiles derived with the assumptions of the uniform film thickness and linear partition equilibrium were in relatively good agreement with the experimental data for the combined continuous and preparative chromatographic system, and it could be used as a powerful predictive tool for determining the optimum operating conditions.

INTRODUCTION

Since the introduction of gas-liquid chromatography, it was recognized that this technology could be used for quantitative separation on an industrial scale. Generally the chromatographic processes fall into two main categories, batch and continuous. The batch type of the processes was initiated in 1953 and commercial units are now available [1]. The continuous system was introduced soon after 1955 and recently concerns on this system have been concentrated mainly to increase the throughputs [2,3].

The principles of the combined continuous and preparative chromatographic system are based on switching the configuration of the columns [4-6]. The less-absorbed component can be obtained purely before the elution of the more-absorbed component in one of the sections (partition section). During that time, in the other section (desorption section) the less-absorbed component remained in the column with the more-absorbed component can be separated by adjusting the additional column length and desorbent velocity. If the above two steps can be simultaneously completed within a certain time (switching time), the feed mixture can be separated continuously. The switching time is varied by the characteristic combination of the stationary liquid and the feed mixtures. In the desorption section, the remained components should be separated within the switching time by change of the operating conditions.

The basic principle of the UOP process [7] is that the components are separated in a rectification zone by a displacement method. In this system which is composed of two sections, however, the components which are not separated in one section can be separated by increasing the column length in the other section. It is evident that the chromatographic system can be extended to more applicability than the UOP process by the suitable selection of a stationary liquid phase. Only a few researchers have roughly reported the experimental results of the continuous or semi-continuous chromatographic systems [8,9].

Using the mathematical models developed for this chromatographic system, the effects of the experimental operating conditions on the elution profiles of the two components will be discussed. Also, the purpose of this work is to compare the experimental data with the calculated values for confirming the usefulness of the models.

*To whom all correspondence should be addressed.

MATHEMATICAL MODELS

The distribution of the stationary liquid phase on the solid support appears to be very complex because of irregularity of pore size and shape. The assumptions for establishing the governing equations of the processes are a uniformly distributed stationary liquid phase on the surface of the inert solid particle, the linear partition isotherm, the negligible sorption and pressure drop effects, and the sphere of a solid particle [4,5,10,11]. As the concept of the uniform film thickness simplifies the phenomena of the porous particle coated with the stationary liquid phase, transient material balances of a component are

$$\frac{\partial c}{\partial t}+u\frac{\partial c}{\partial z}=\frac{E}{\epsilon}\frac{\partial^2 c}{\partial z^2}-\frac{3}{r_p}\frac{1-\epsilon}{\epsilon}D_e\frac{\partial q}{\partial r}\Big|_{r=r_p} \tag{1}$$

for the mobile phase,

$$\epsilon_p\frac{\partial q}{\partial t}=D_e\frac{1}{r^2}\frac{\partial}{\partial r}\left(r^2\frac{\partial q}{\partial r}\right)-A_p k_g\left(q-\frac{n|_{x=\delta}}{K}\right) \tag{2}$$

for the intraparticle phase, and

$$\frac{\partial n}{\partial t}=D_i\frac{\partial^2 n}{\partial x^2} \tag{3}$$

for the stationary liquid phase.

The initial and boundary conditions are:

$$c=q=n=0 \qquad (\text{for } t=0,\ z>0) \tag{4}$$

$$c=c_0(t) \qquad (\text{for } t>0,\ z=0) \tag{5}$$

$$c=\text{finite} \qquad (\text{for } t>0,\ z\to\infty) \tag{6}$$

$$\frac{\partial q}{\partial r}=0 \qquad (\text{for } t>0,\ r=0) \tag{7}$$

$$\frac{\partial n}{\partial x}=0 \qquad (\text{for } t>0,\ x=0) \tag{8}$$

$$D_e\frac{\partial q}{\partial r}=k_f(c-q) \qquad (\text{for } t>0,\ r=r_p) \tag{9}$$

$$D_i\frac{\partial n}{\partial x}=k_g\left(q-\frac{n}{K}\right) \qquad (\text{for } t>0,\ x=\delta). \tag{10}$$

It is assumed that the partition effect is dominant to that of adsorption with a linear equilibrium isotherm. The solution Eq. (1) to Eq. (10) in the Laplace domain is

$$C(s)=C_0(s)\exp\left(\frac{L}{2}\left[\frac{u_0}{E}-\left\{\left(\frac{u_0}{E}\right)^2+4\lambda\right\}^{1/2}\right]\right) \tag{11}$$

at the bed exit, z = L, where

$$\lambda=\frac{\epsilon}{E}\left(s+\frac{3(1-\epsilon)}{r_p\epsilon}k_f\left\{1-\frac{\sinh(\lambda_2 r_p)}{r_p\lambda_1}\right\}\right) \tag{12}$$

$$\lambda_1=\frac{r_p k_f}{D_e\lambda_2\cosh(\lambda_2 r_p)+\left(k_f-\frac{D_e}{r_p}\right)\sinh(\lambda_2 r_p)} \tag{13}$$

$$\lambda_2=\left(\frac{1}{D_e}\left\{\epsilon_p s+A_p k_g\left\{1-\frac{A_p k_g^2\cosh\lambda_3}{D_e K\sqrt{\frac{s}{D_i}}\lambda_3+D_e k_g\cosh\lambda_3}\right\}\right\}\right)^{1/2} \tag{14}$$

$$\lambda_3=\delta\sqrt{\frac{s}{D_i}}\ . \tag{15}$$

The usual method of operating fixed beds for preparative scale is to use a large pulse of feed input to the column followed by a longer period of flow of carrier gas. In case of pulse input, $C_0(s)$ has the following form:

$$C_0(s)=\frac{1-e^{-st_0}}{s} \tag{16}$$

where t_0 = time of feed-injection, then Eq. (11) becomes

$$C(s)=\frac{1-e^{-st_0}}{s}\exp\left(\frac{L}{2}\left\{\frac{u_0}{E}-\left[\left(\frac{u_0}{E}\right)2+4\lambda\right]^{1/2}\right\}\right) \tag{17}$$

Equation (17) can be used to predict the concentration profile of the component in the partition section. It is assumed that in the desorption section the components are partitioned initially with the inlet concentration of the feed, c_0. The governing equations are same as in the partition section. However, some of initial and boundary conditions are different from those of the partition section. The initial condition and the boundary condition in the desorption section are as follows:

$$c=q=c_0 \qquad (\text{for } t=0,\ z>0) \tag{18}$$

$$n=Kc_0 \qquad (\text{for } t=0,\ z>0) \tag{19}$$

$$c=0 \qquad (\text{for } t>0,\ z=0). \tag{20}$$

Under the condition, the solution in the Laplace domain is

$$C(s)=\gamma\left(\exp\left\{\frac{L}{2}\left(\frac{u_0}{E}-\left[\left(\frac{u_0}{E}\right)+4\gamma_1\right]^{1/2}\right)\right\}-1\right) \tag{21}$$

where

$$\gamma=\left(-\frac{\epsilon_p c_0}{E}+\frac{3(1-\epsilon_p)}{r_p E}k_f\left\{\frac{\gamma_2\sinh(\sqrt{\gamma_4}r_p)}{r_p}+\frac{\gamma_5}{\gamma_4}\right\}\right)/\gamma_1 \tag{22}$$

$$\gamma_1=\left(-\frac{\epsilon s}{E}+\frac{3(1-\epsilon)}{r_p E}k_f\left\{1-\frac{\gamma_3\sinh(\sqrt{\gamma_4}r_p)}{r_p}\right\}\right) \tag{23}$$

Table 1. The kinetic constant and other parameters used in the simulations

mesh size	60/80		45/60	20/30
r_p (m)	0.0000996		0.000136	0.000314
20% liquid loading ϵ_p	0.66		0.66	0.54
20% liquid loading δ (μm)	0.0955			
DEE temperature °C	D_l 10^{-10} m^2/sec	K	DCM D_l 10^{-10} m^2/sec	K
25	0.471	184.2	0.595	437.1
35	0.650	126.3	0.901	297.1
45	1.090	88.7	1.275	206.8
A_p (m^2/m^3)	1300000.0			
ϵ	0.41			
D_e ($\times 10^{-9}$ m^2/sec)	1.00 (DEE)		2.00 (DCM)	

$$\gamma_2 = -\gamma_5 k_f/\gamma_4 (D_e \sqrt{\gamma_4} r_p \cosh(\sqrt{\gamma_4} r_p) - \sinh(\sqrt{\gamma_4} r_p))/r_p^2 + k_f \sinh(\sqrt{\gamma_4} r_p)/r_p) \quad (24)$$

$$\gamma_3 = \frac{-\gamma_4}{\gamma_5 \gamma_2} \quad (25)$$

$$\gamma_4 = \frac{1}{D_e}(\epsilon_p s + A_p k_g) - \frac{A_p k_g^2 \cosh\left(\sqrt{\frac{s}{D_l}}\delta\right)}{D_e K \sqrt{D_l s} \sinh\left(\sqrt{\frac{s}{D_l}}\delta\right) + k_g \cosh\left(\sqrt{\frac{s}{D_l}}\delta\right)/K} \quad (26)$$

$$\gamma_5 = \frac{A_p k_g}{D_e K}\left\{\frac{Kc_0}{s} - \frac{\frac{k_g c_0}{s}\cosh\left(\sqrt{\frac{s}{D_l}}\delta\right)}{\sqrt{D_l s}\sinh\left(\sqrt{\frac{s}{D_l}}\delta\right) + k_g \cosh\left(\sqrt{\frac{s}{D_l}}\delta\right)/K}\right\} + \frac{c_0}{D_e}. \quad (27)$$

Equation (17) is used as the input function for the inlet of the additional column of the desorption section. That is

$$c_0(s) = \gamma\left(\exp\left\{\frac{L}{2}\left(\frac{u_0}{E} - \left[\left(\frac{u_0}{E}\right)^2 + 4\gamma_1\right]^{1/2}\right)\right\} - 1\right). \quad (28)$$

The governing equations, initial conditions and boundary conditions are same as those in the partition section. Therefore, the solution of the desorption section with the additional column length (L') in the s-domain is

$$C(s) = \gamma\left(\exp\left\{\frac{L}{2}\left(\frac{u_0}{E} - \left[\left(\frac{u_0}{E}\right)^2 + 4\gamma_1\right]^{1/2}\right)\right\} - 1\right) \times \exp\left(\frac{L'}{2}\left\{\frac{u_0}{E} - \left[\left(\frac{u_0}{E}\right)^2 + 4\lambda\right]^{1/2}\right\}\right). \quad (29)$$

The resulting Laplace transformed equations (Eqs. (17), (21) and (29)) should be converted into the real time domain, but the analytical method is highly unlikely possible. For an approximation technique, the equations are inverted numerically with the curve fitting procedure suggested by Dang and Gibilaro [12]. In the numerical inversion, the infinite upper integration limit is taken as the corresponding value of the frequency to the amplitude ratio of the Laplace transformed equations of 0.0001, and it takes just several minutes using IBM AT^{TM} to transform the equations into the real time domain. The kinetic constant and other parameters used in the simulations are listed in Table 1 [4,5].

EXPERIMENTAL

Diethylether (DEE) and dichloromethane (DCM) were used as the feed mixtures, and their boiling points are 37.8°C and 34.6°C, respectively. The partition coefficients of DEE and DCM were evaluated on an analytical chromatographic column over the wider

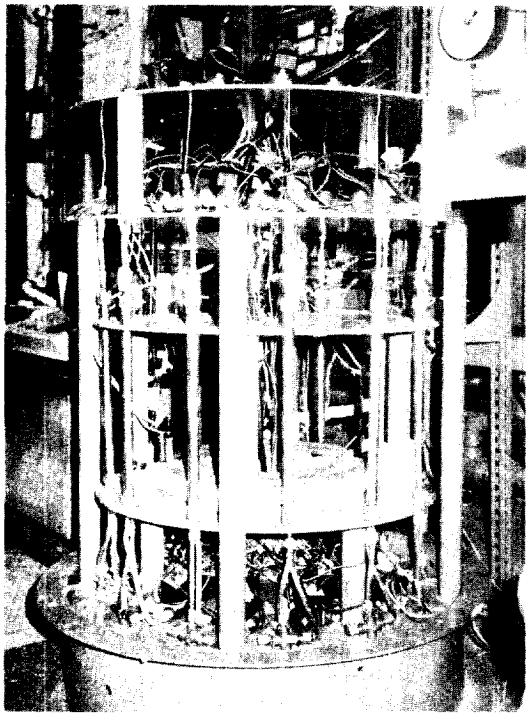

Fig. 1. Photograph of the main chromatographic unit.

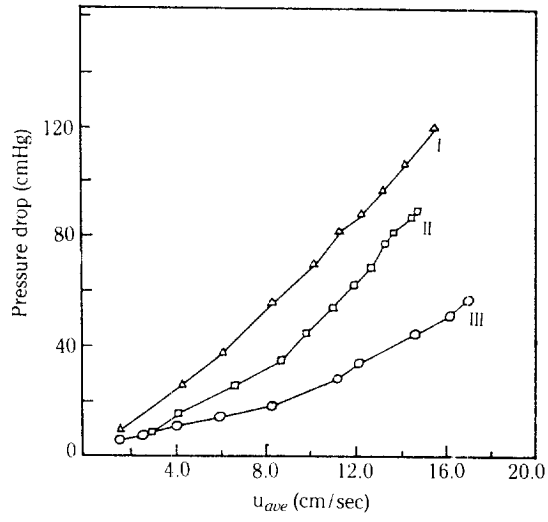

Fig. 2. Effect of particle size on pressure drop.
(I); 60/80 mesh, L = 100 cm, (II); 20/30 mesh, L = 200 cm, (III); 20/30 mesh, L = 100 cm

temperature ranges [13]. Nitrogen was used as the carrier gas and the desorbent.

Twelve columns were arranged in a circular form. The column was made of stainless steel, 1 cm i.d., 30 cm height, and the packed height was 25 cm. In both ends of the column, glass wool was used for solid particles retained in place. The column was packed with Chromosorb A (Alltech Associates) which has good capacity to load stationary liquid and the surface is not highly adsorptive, so it is mainly used for preparative-scale separation [14]. The Chromosorb A of three different particle sizes used were of 60/80, 45/60, and 20/30 mesh commercially available. A rotavapor (Brinkmann Co.) was used to coat dinonylphthalate on the particle, and the ratio of the stationary liquid to the solid support was 0.20 by weight fraction for all particle sizes. Each column has four openings, two for entering streams and two for withdrawing streams, and it was covered with ceramic insulation to keep the column temperature constant.

Photograph of the main chromatographic system was shown in Fig. 1 [4-6]. Five solenoid valves (CKD, AB 31-01-4) were arranged around a column. A supporter was made to fix the twelve columns, sixty solenoid valves, and four distributors, and was enclosed with the covers to maintain the desired temperature in the system. The four distributors, two for entering streams and two for withdrawing streams, were installed. Each distributor formed a cylindrical type whose upper side had one central bore, and the side of the distributor had twelve screwed openings. The entering stream passed through the central bore and went into one of the openings in the distributor, and then it entered the inlet of the column through the solenoid valve connected with the opening. Conversely, the withdrawing stream through the solenoid valve from the outlet of the column went through one of the openings and the central bore in the distributor, and finally this was sent for analysis.

Two outlet streams and inlet feed mixtures were analyzed by a conventional gas chromatograph (Gow Mac 550P thermal conductivity detector) with a syringe (Hamilton Co.) and a ten-port multi-functional sampling valve (Valco Instruments Co.). Pressure gauges were set at the inlet and outlet of the main system, so the pressure drops of the two sections were recorded. The dead volume of the system was determined from the measurement of the retention time of a helium sample.

The sixty solenoid valves in the main chromatographic system were controlled by a programmable controller. Flow paths of the partition and desorption section were initially set by the controller, and then they were automatically and consecutively turned to the next step after a switching time.

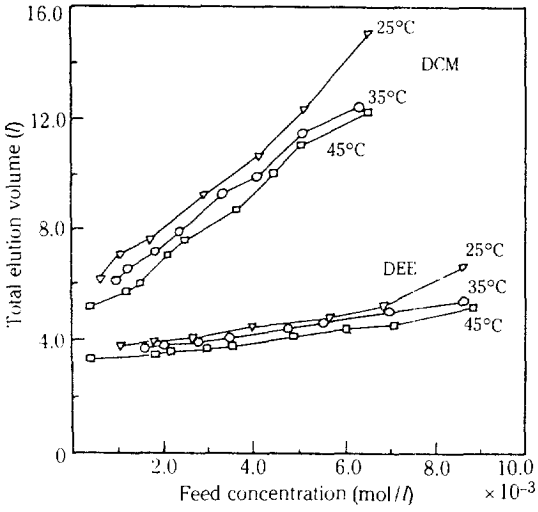

Fig. 3. Effect of feed concentration on total elution volume with column temperatures.

20/30 mesh, u_{ave} = 9.53 cm/sec, L = 100 cm, 300 sec of switching time

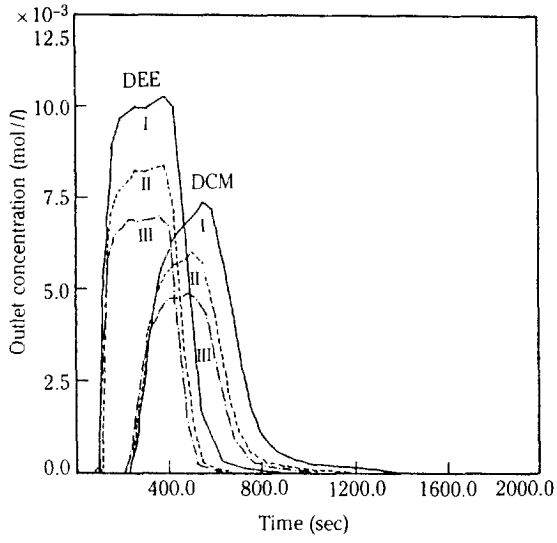

Fig. 4. Effect of feed concentration on elution profile.

(I); $c_{0,DEE} = 10.0 \times 10^{-3}$ mol/l, (II); 8.3×10^{-3} mol/l, (III); 6.8×10^{-3} mol/l, (I); $c_{0,DCM} = 7.3 \times 10^{-3}$ mol/l, (II); 6.3×10^{-3} mol/l, (III); 4.9×10^{-3} mol/l, 20/30 mesh, 25°C, u_{ave} = 9.53 cm/sec, L = 100 cm, 300 sec of switching time

RESULTS AND DISCUSSION

In a gas chromatographic column, the gas flows through the narrower interstices between solid supports packed in the column. The local changes in the viscosity and flow velocity of the gaseous mixture result in the pressure gradient along the column [15]. The smaller particles caused the higher pressure drop as shown in Fig. 2. The velocity gradient would be changed by the consequence of the pressure changes in the column. The averae velocity in abscissa of the figure, u_{ave}, means the velocity corrected by the following compressibility factor suggested by James and Martin [16],

$$J = \frac{3((P_i/P_0)^2 - 1)}{2((P_i/P_0)^3 - 1)} \quad (30)$$

where P_i and P_0 denote the inlet and outlet pressure, respectively. Pressure drop of 30-90 cmHg was observed in the experimental ranges of this system. The gas velocity will be more uniform at a low inlet-to-outlet pressure ratio. Therefore, it is desirable to use rather larger particle size and lower flow rates of carrier gas or desorbent in order to separate the feed efficiently.

The total elution volumes of the mixture, DEE and DCM, are plotted with the feed concentration and the column temperature in Fig. 3. This volume is the quantity of the gas volume which can elute the components completely in the length of the column. Also in the figure, the slope of each component is distinguishable. Although the slope of the elution profile of DEE is low and that of DCM is high, the bandwidth of the both components was observed to be wider with

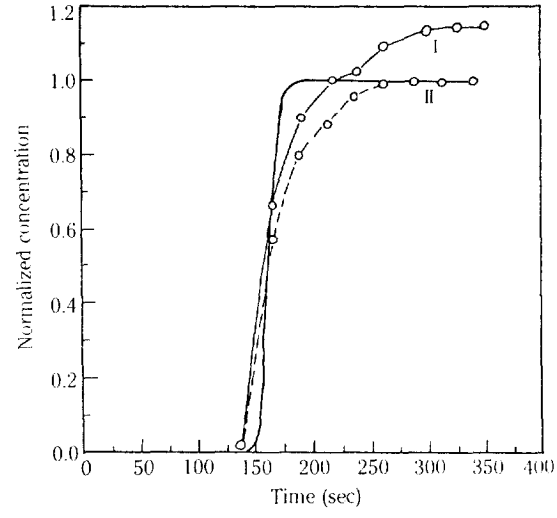

Fig. 5. Comparison of experimental data (○) with calculated values (—) for DEE.

(I); $c_{0,DEE} = 0.90 \times 10^{-3}$ mol/l, (II); 0.91×10^{-3} mol/l, (I); $c_{0,DCM} = 3.40 \times 10^{-3}$ mol/l, (II); 0.90×10^{-3} mol/l, 20/30 mesh, 35°C, u_{ave} = 9.10 cm/sec, L = 150 cm, 360 sec of switching time

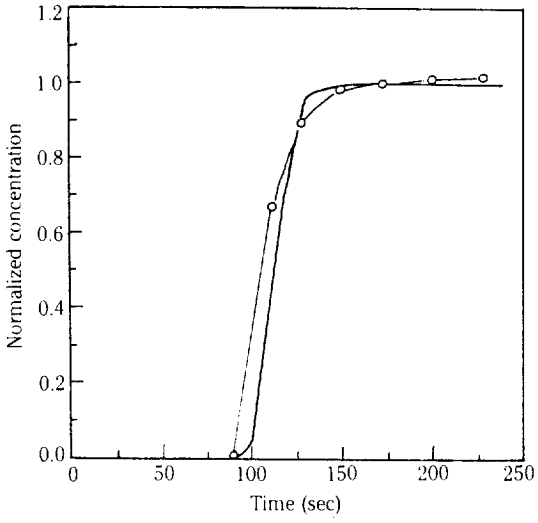

Fig. 6. Comparison of experimental data (○) with calculated values (—) for DEE.
$c_{0,DEE} = 0.98 \times 10^{-3}$ mol/l, $c_{0,DCM} = 0.91 \times 10^{-3}$ mol/l, 45/60 mesh, 35°C, $u_{ave} = 8.80$ cm/sec, L = 100 cm, 240 sec of switching time

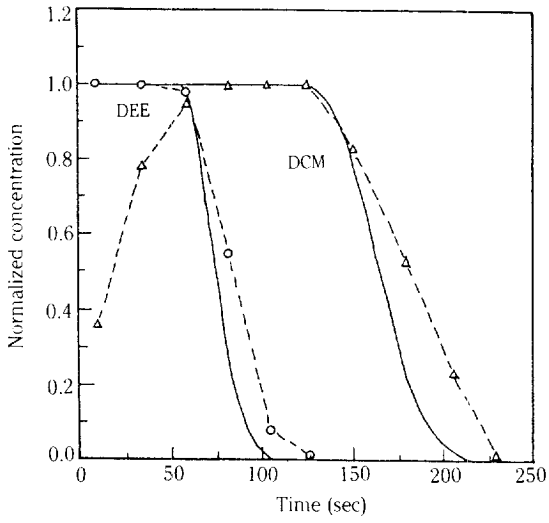

Fig. 7. Comparison of experimental data of DEE (○) and DCM (△) with calculated values (—).
$c_{0,DEE} = 0.98 \times 10^{-3}$ mol/l, $c_{0,DCM} = 0.82 \times 10^{-3}$ mol/l, 20/30 mesh, 35°C, $u_{ave} = 20.50$ cm/sec, L = 100 cm, 240 sec of switching time

Table 2. Switching times with operating conditions

(unit: sec)

mesh size	20/30		45/60		60/80	
T(°C) L(cm)	100	150	100	150	100	150
25	270	480	300	480	300	480
35	240	360	240	360	240	360
45	180	270	180	300	180	300

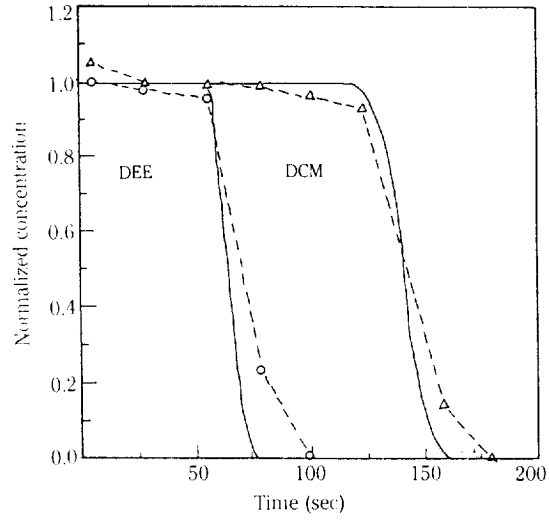

Fig. 8. Comparison of experimental data of DEE (○) and DCM (△) with calculated values (—).
$c_{0,DEE} = 0.94 \times 10^{-3}$ mol/l, $c_{0,DCM} = 0.78 \times 10^{-3}$ mol/l, 45/60 mesh, 45°C, $u_{ave} = 11.30$ cm/sec, L = 100 cm, 180 sec of switching time

increasing the feed concentration and decreasing the column temperature which was resulted from the limited capacity of vaporization when the more feed mixtures were injected (see Fig. 4). c_0 indicates the inlet concentration of the feed.

The calculated curves in the following figures were the numerical inversion of Eqs. (17), (21) and (29), with the partition section, the desorption section, and the desorption section with additional column length, respectively. The two experimental concentration profiles with the feed concentration of DEE are compared to the calculated values in the partition section as in Fig. 5. At the higher concentration of DCM, the normalized concentration exceeded the inlet feed concentration of the DEE. For the particle size of 20/30 mesh, the leading edge of the experimental profile was less steep than that of the calculated, however for 45/60 mesh, the agreement between the two profiles was good, as shown in Fig. 6. The deviation in Fig. 5 may be attributed to the larger axial dispersion of the particle size, 20/30 mesh. The performance of the system in the partition section was not varied greatly by the effect of the particle sizes, because the switching time was almost constant for the particle sizes involved (see Table 2).

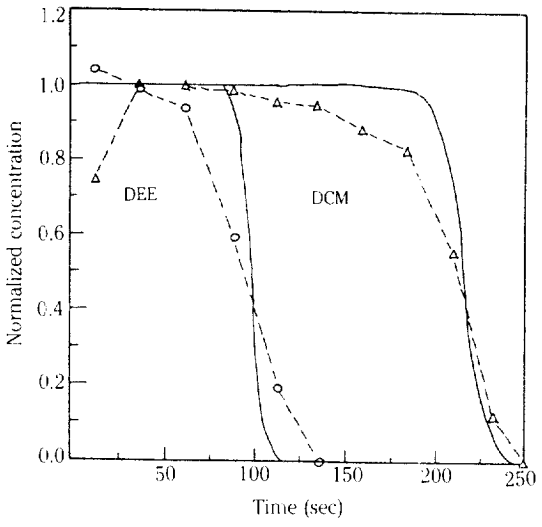

Fig. 9. Comparison of experimental data of DEE (○) and DCM (△) with calculated values (—).
$c_{0,DEE} = 0.94 \times 10^{-3}$ mol/l, $c_{0,DCM} = 0.75 \times 10^{-3}$ mol/l, 45/60 mesh, 45°C, $u_{ave} = 11.10$ cm/sec, L = 150 cm, 300 sec of switching time

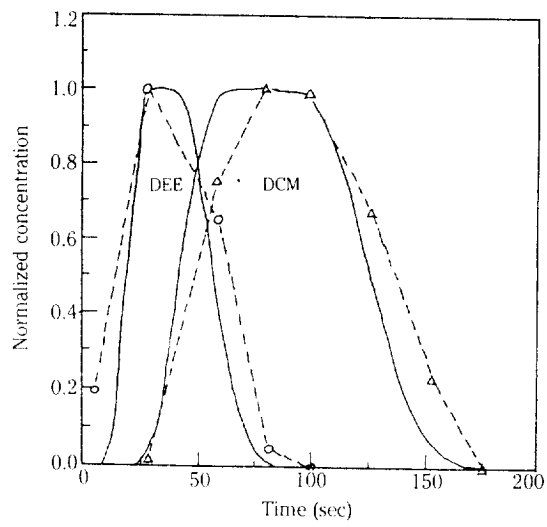

Fig. 10. Comparison of experimental data of DEE (○) and DCM (△) with calculated values (—).
$c_{0,DEE} = 0.61 \times 10^{-3}$ mol/l, $c_{0,DCM} = 0.57 \times 10^{-3}$ mol/l, 20/30 mesh, 45°C, $u_{ave} = 18.60$ cm/sec, L = 100 cm, L' = 50 cm, 240 sec of switching time

Figure 7 shows the concentration profiles of the desorption section. In the model equations (Eqs. (18), (20)), the initial concentrations were assumed to be distributed with the inlet concentration of the feed, c_0. This assumption seems to be valid for the less-absorbed component (DEE) but the more-absorbed component (DCM) is not exactly for the case. That is, in the partition section which is to become the desorption section after a switching time, DCM is not uniformly distributed and more likely maldistributed around the inlet of the column, because its partition coefficient is large. Therefore, during the next switching time, the concentration profile of DCM in the desorption section deviates from the calculated values as in Fig. 7. However, as the column temperature increased, such deviation between the calculated values and experimental data for the leading edge in the profile of DCM was negligible due to the good distribution in the higher temperature (see Fig. 8).

Figure 9 shows the more skewed experimental profiles in the longer column length of 150 cm. This tendency seems to be due to the increased axial dispersion caused by the higher outlet gas velocity [10]. The average gas velocities, u_{ave}, used in Figs. 8 and 9 were almost same, however, the factor of J was 0.593 in the column length of 150 cm, while it was 0.728 in the length of 100 cm. It means that the outlet gas velocity of the longer column, 18.7 cm/sec, is much higher than that of the shorter column, 15.5 cm/sec.

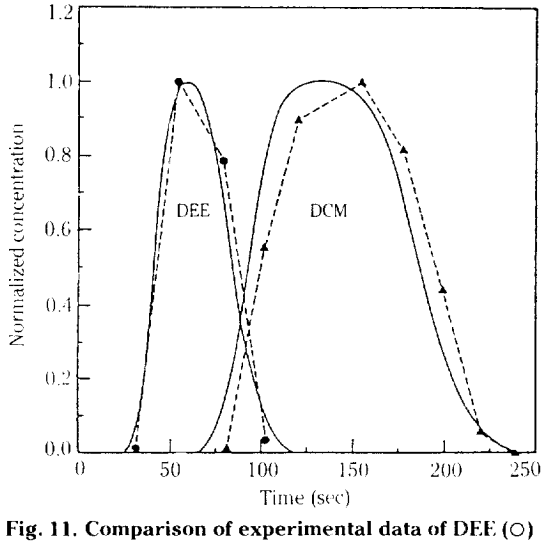

Fig. 11. Comparison of experimental data of DEE (○) and DCM (△) with calculated values (—).
$c_{0,DEE} = 0.61 \times 10^{-3}$ mol/l, $c_{0,DCM} = 0.57 \times 10^{-3}$ mol/l, 20/30 mesh, 35°C, $u_{ave} = 19.90$ cm/sec, L = 100 cm, L' = 100 cm, 240 sec of switching time

The two components were not resolved in the desorption section as shown in Figs. 7-9. If the desorption section is used exclusively, the more-absorbed component can be obtained purely after the unseparated mixture are recycled in a batch type. Continuous operation, however, can be achieved by connecting

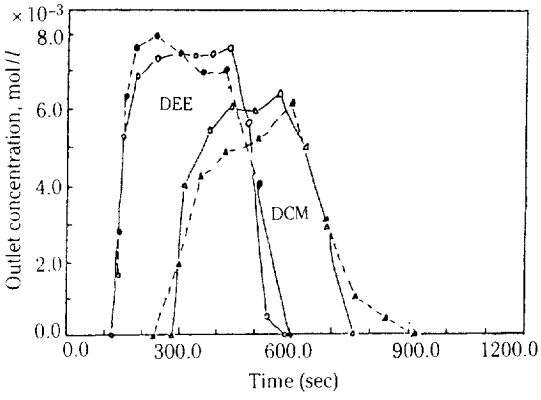

Fig. 12. Comparison of experimental data of DEE (○) and DCM (△) in pure components with those of DEE (●) and DCM (▲) in their mixtures.
for pure component, $c_{0,DEE} = 6.81 \times 10^{-3}$ mol/l, $c_{0,DCM} = 5.19 \times 10^{-3}$ mol/l, for mixtures, $c_{0,DEE}$ 7.06×10^{-3} mol/l, $c_{0,DCM} = 5.46 \times 10^{-3}$ mol/l, 20/30 mesh, 35°C, $u_{av} = 6.30$ cm/sec, L = 75 cm, 360 sec of switching time

the additional columns to the end of the desorption section. As shown in Figs. 10 and 11, the resolution between the two components was improved gradually by increasing the additional column length from 50 to 100 cm. The small differences in the trailing edge of the concentration profile of DEE and in the leading edge of DCM may be partly caused by the assumption of the linear partition equilibrium. With adjustment of the desorbent velocity alone, the remained components in the desorption section with the additional column length can be separated within the switching time of 240 sec (Fig. 11).

When the feed concentration is increased, the mechanism in the column becomes more complex, and generally the information about the nonlinear isotherms is necessary to develop the model equations. Despite of the relatively high concentration of the feed, the differences between the elution profiles of pure materials and mixtures were not large as shown in Fig. 12. The interaction between the components seems to be negligible within the range of the concentration of the experiments. The pressure drop by the smaller particle size and longer column length caused the variation of the gas velocity, and the higher feed concentrations along the length of the column was necessarily accompanied by change of the velocities. In this system, the assumption that the velocity of carrier or desorbent remained constant throughout the column was compensated by the average gas velocity. In spite of the small deviations, the calculated concentration profiles are in relatively good agreement with the experimental data. Hence, the uniform thickness model can be used as a suitable estimation of the optimum operating conditions for the combined continuous and preparative chromatographic system.

CONCLUSIONS

Based on the operational principle of the combined continuous and preparative chromatographic system, the experimental conditions were mainly affected by the additional column length and the desorbent velocity. The increased pressure drop caused by the longer column length and higher gas velocity could be minimized by using larger particles, and the variation of the velocity along the column was simply corrected by the average gas velocity. Because the differences between the elution profiles of the pure materials and mixtures were relatively small in this gas-liquid chromatography, the assumption of linear partition relation was reasonable.

The switching time for good separation was experimentally determined, and it was mainly affected by the column temperature and column length. In spite of the small deviations caused by the assumptions of the constant gas velocity and linear partition isotherm, the theoretical concentration profiles were in relatively good agreement with the experimental data. For the combined continuous and preparative chromatographic system, therefore, the uniform thickness model can be used for the proper estimation of optimum operating conditions.

NOMENCLATURE

A_p : surface area of porous particle per unit volume [m^2/m^3]
c : concentration of solute in mobile phase [mol/l]
c_0 : inlet concentration of solute [mol/l]
C(s) : Laplace transform of c(t)
D_e : diffusion coefficient in pore spacing [m^2/sec]
D_l : diffusion coefficient in stationary liquid phase [m^2/sec]
E : axial dispersion coefficient [m^2/sec]
k_f : interparticle mass transfer coefficient [m/sec]
k_g : intraparticle mass transfer coefficient with respect to stationary liquid phase-film [m/sec]
J : compressibility factor defined in Eq. (30)
K : partition coefficient
L : column length in partition section and desorption section [cm]
L' : additional column length in desorption section

[cm]

n : concentration of solute in stationary liquid phase [mol/l]

P_i : pressure at inlet condition [cmHg]

P_0 : pressure at outlet condition [cmHg]

q : concentration of solute in pore spacing [mol/l]

r : radial distance [m]

r_p : radius of porous particle [m]

s : variable of Laplace transform

t : time [sec]

t_0 : time of feed-injection [sec]

T : column temperature [K]

u : interstitial velocity of carrier gas or desorbent [cm/sec]

u_0 : superficial velocity of carrier gas or desorbent [cm/sec]

u_{ave} : average velocity of carrier gas or desorbent [cm/sec]

x : distance perpendicular to surface of porous particle [m]

z : axial distance [m]

Greek Letters

γ, γ_1, γ_2, γ_3, γ_4, γ_5 : values defined by Eq. (22) to Eq. (27)

δ : film thickness of stationary liquid phase [μm]

ϵ : void fraction of chromatographic column

ϵ_p : porosity with presence of stationary liquid phase

λ, λ_1, λ_2, λ_3 : values defined by Eq. (12) to Eq. (15)

REFERENCES

1. Bonmati, R.G., Chapelet-Letourneux, G. and Margulis, J.R.: *Chem. Eng.*, **87,** 70 (1989).
2. Barker, P.E.: "Developments in Chromatography", Knapman, C.H. (Editor), Applied Science Publisher, London (1978).
3. Grushka, E. (Editor): "Preparative-Scale Chromatography", Marcel Dekker, Inc., New York and Basel (1989).
4. Row, K.H.: Ph.D. Thesis, Korea Advanced Institute of Science & Technology, Seoul (1986).
5. Row, K.H. and Lee, W.K.: "Separation by Gas-Liquid Chromatography", Cheremisinoff, N.P. (Editor), Handbook of Heat and Mass Transfer, Vol. 3: Catalysis, Kinetics, and Reactor Engineering, Chapter 22, Gulf Publishing Company, Houston (1989).
6. Row, K.H. and Lee, W.K.: *Sep. Sci. and Technol.*, **22,** 1761 (1987).
7. Broughton, D.B.: *Chem. Eng. Pro.*, **64,** 60 (1969).
8. Ching, C.B. and Ruthven, D.M.: *Chem. Eng. Sci.*, **40,** 1411 (1985).
9. Fish, B.B., Carr, R.W. and Aris, R.: *AIChE J.*, **35,** 737 (1989).
10. Row, K.H. and Lee, W.K.: *J. Chem. Eng. Japan*, **19,** 173 (1986).
11. Alkarasani, M.A. and McCoy, B.J.: *Chem. Eng. J.*, **23,** 81 (1982).
12. Dang, N.D.P. and Gibilaro, L.G.: *Chem. Eng. J.*, **8,** 157 (1974).
13. Moon, I., Row, K.H. and Lee, W.K.: *Korean J. Chem. Eng.*, **2,** 155 (1985).
14. McNair, H.M. and Bonelli, A.J.P.: "Basic Gas Chromatography", Varian Aerograph, Berkeley (1969).
15. Littlewood, A.: "Gas Chromatography", Academic Press, New York (1970).
16. James, A.T. and Martin, A.J.P.: *Analyst*, **77,** 915 (1952).
17. Row, K.H.: *Chromatographia*, **25,** 961 (1988).